Nanoparticle Synthesis of Titanium Silicalite for Fiber, Film, and Monolith Formation

K. T. Jung, J. H. Hyun, and Y. G. Shul
Dept. of Chemical Engineering, Yonsei University, 120-749, Seoul, Korea

K.-K. Koo
Dept. of Chemical Engineering, Sogang University, 121-742, Seoul, Korea

Zeolite fiber, film, and monolith were prepared by using nanosize titanium silicalite (TS-1) crystals. Films and fibers of TS-1 zeolite were optically transparent, which might be important for advanced optozeolitic materials. A permeation result of gases on monolith indicates that the gas permeation is governed by the Knudsen mechanism. All types of TS-1 zeolites manufactured in this work are observed to be MFI structure with an orthorhombic symmetry. These results suggest that nanosize zeolites have potential to allow morphological design with applications for advanced functional materials.

Introduction

Sol-gel processing is used for synthesis of various types of advanced materials (Brinker and Scherer, 1990). This method allows for preparation at room temperature of solid gel from molecular precursors in solution. Inorganic salts or metal organic compounds are dissolved in solvents and then sols are formed with fine inorganic particles composed of metal–oxygen–metal bonds. Fabrication of ceramics, glass, and composites of various shapes results from the molecular manipulation and control of homogeneous structures in the sol state.

The shape of the final product depends on the control of the sol state, that is, the size and morphology of particles in the dispersed phase. In general, nanosized particles are dispersed in the liquid solution. From this controlled sol state, fiber, film, and monolith formations are feasible. For example, gel fibers are drawn from the viscous sol when metal oxide particles produced in the sol have long shapes and the sol exhibits transformation from Newtonian to thixotropic fluid behavior (Grassi et al., 1996). The formation of films is also dependent on the particle size, particle-size distribution, and the extent of branching (or aggregation) of the particles. The synthesis of self-aligned materials by the control of particle size and morphology in the sol state has also been studied in the colloid system. Nanosized gold and silica particles as well as latex colloid particles dispersed in water are used in the film formation for data storage, optical devices, and microelectronics (Lin et al., 1989).

For more than a century, extensive studies on zeolites, which are generally characterized as having large internal surface areas and well-defined pore systems, have been made as sorbents, ion-exchange materials, and catalysts (Breck, 1974). However, most research on zeolites has been limited to the synthesis of zeolites with new structures or to the study of reactions using pelletized or granular forms of the zeolites. In recent years, several studies on the morphological design of zeolites as fibers, films, and monoliths have been reported (Hennepe et al., 1987; Jia et al., 1994). Valchev et al. (1990) suggested the *in situ* synthesis of zeolite on mullite fiber to minimize pressure drop. Polyamide fiber containing 10 wt % zeolite has been synthesized for the application of zeolite fibers to antibacterial wool (Hayashi et al., 1992). Zeolite membranes have been made by *in situ* crystallization of zeolites on substrates or by incorporating the zeolite crystals in polymeric matrices, such as silicone rubber, or in a glassy silica matrix (Sano et al., 1992; Dong et al., 1992). Monolithic zeolites have also been prepared by coating zeolite particles on the preshaped monolith (Farrauto and Voss, 1996; Yan et al., 1995).

However, there are few attempts to design the zeolite morphology by controlling size of zeolite, especially by using nano-sized zeolite as in sol-gel process. Nano-sized zeolites has been obtained by some investigators (Hoffman et al., 1992; Scheoman et al., 1994; Lovallo and Tsapatsis, 1996a; Persson et al., 1995), but they did not control the size of the zeolite nor the morphology of the nanosized zeolite. Recently, Tsapatsis et al. (1995) have synthesized nanosized zeolite L, and they have made zeolite film by using the small size of the nanoparticles.

In this study, nanosized titanium silicalite (TS-1) was prepared with similar conditions as for the synthesis of ZSM-5 (Kiyozumi et al., 1996a). The formation of zeolite fiber, film, and monolith was attempted by controlling the particle size and process to get a designed morphology. The physicochemical characterizations of these samples are discussed in this article.

Materials and Method

Chemicals

Tetraethylorthosilicate (TEOS, Aldrich), titanium butoxide (Aldrich), and 20% aqueous tetrapropylammonium hydroxide (TPAOH, Aldrich) solution were used without further purification for Si and Ti precursor and template, respectively. First-grade isopropyl alcohol and hydrogen chloride (Yakuri) were used without purification. The water used as dilute solvent was purified by means of a Millipore filtration device (ELGA STAT, UHQ).

Apparatus and procedure

TS-1 zeolite was prepared by a similar method given in the literature (Thangaraj et al., 1992; Jung et al., 1996a). To obtain nanosized crystals, TS-1 zeolite was crystallized at 80°C and atmospheric pressure for 50–100 h. TEOS and TPAOH solutions were well mixed by agitation. Separately, titanium butoxide was diluted with isopropyl alcohol and this solution was then slowly stirred into the mixture of TEOS and TPAOH. Thereafter, the reaction mixture was heated to a temperature of about 80°C for 2 h to eliminate the alcohol. After the removal of alcohol, deionized water was added to the reaction mixture. The composition of the initial reaction mixture in terms of molar ratio is as follows:

$$Ti:Si:H_2O:TPAOH:\text{isopropanol} = 0.03:1:25:0.32:0.77.$$

The clear mixture was heated in a polypropylene bottle submerged in a silicone oil bath preheated to 80°C under reflux conditions while stirring. During the crystallization of TS-1 zeolite, the particle size of TS-1 was monitored by using dynamic light scattering (DLS). TS-1 solid phase was separated from the extracted mother solution by centrifugation. Figure 1 shows the preparation procedures for various zeolite shapes. After separating the nanosized TS-1 particles, they were redispersed in deionized water with a concentration of 0.5–20.0% (w/w). The dispersed solution was transferred to a glass test tube and dried for 10 h at 100°C to form TS-1 fiber (FTS-1). In the case of TS-1 zeolite film, microslide glass was immersed in the dispersed TS-1 solution and dried at 100°C.

For the preparation of monolith, the precursor was prepared by the method given by Uguina et al. (1995). First, TEOS is hydrolyzed at room temperature with 0.05 M HCl aqueous solution. Titanium butoxide dissolved in isopropyl alcohol is then added and hydrolyzed with stirring for slower condensation of the titanium species. After TPAOH is dropped into the mixed clear solution, the solution is converted to a gel. In the present study, before the hydrothermal crystallization, the cogel powder was pelletized to monolithic shape (13 mm × 1.5 mm diameter and thickness, respectively). And it was transferred to autoclave and crystallized at 170°C for 3 days under hydrothermal conditions.

Characterization

X-ray powder diffractiometer (Rikaku) was used to identify the phases present in the TS-1 powders using CuKα radiation ($\lambda = 1.5405$ nm). Fourier transform IR (FT-IR) spectra in the 400–1,500 cm^{-1} range were recorded using a Genesis instrument and the KBr pellet technique. Morphology of the TS-1 crystals and TS-1 fiber were studied by optical microscopy (Nikon, SMZ-2T), scanning electron microscope (JEOL), transmission electron microscopy (Hitachi, H-600), and atomic force microscopy (AFM). Particle-size and particle-size-distribution measurement were performed using dynamic light scattering with a Brookhaven Particle Sizer, Zetaplus, using diluted TS-1 particles in deionized water (0.1 wt%). BET analysis was performed by using the Sorptomatic-1990 Fission, and pore-sized distribution was calculated by the Horvath-Kawazoe method (Elferink et al., 1996).

Results and Discussion

Synthesis of nanosized TS-1 particles and TS-1 zeolite sol

Figure 2 shows the change in particle size and crystallinity of TS-1 particles with the crystallization time at 80°C. X-Ray powder diffraction was used to identify the various phases in

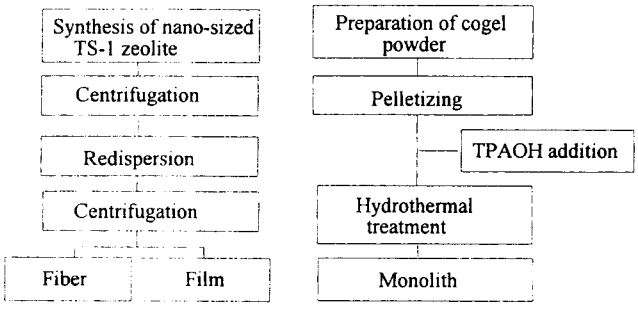

Figure 1. Preparation procedure for fiber, film, and monolith TS-1 zeolite.

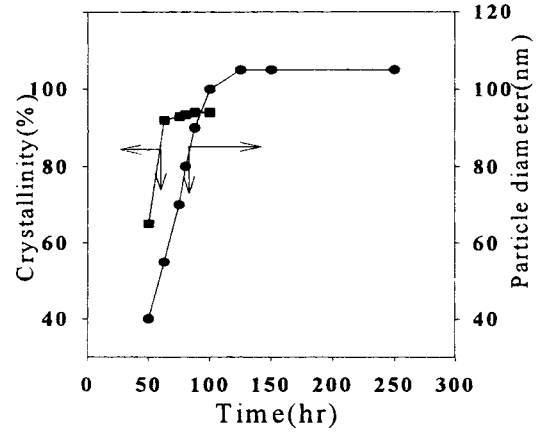

Figure 2. Changes of crystallinity and particle size of TS-1 zeolite (1 atm, 80°C).

the solid fraction. The degree of crystallinity of the TS-1 sample was evaluated by comparing the area of selected peaks ($2\theta = 22-25°$) of the solid product with the reference sample, which is well-crystallized TS-1 zeolite (Mintova et al., 1992).

When crystal formation is beginning, particles of less than 40 nm are generated after a long induction period and grow rapidly up to 110 nm as time passes. The change in particle size follows a typical S-shaped curve generally shown in any other zeolite synthesis (Barrer, 1982). TS-1 particles were separated after 80 h. At this time the crystallinity was about 95%. After separating the TS-1 crystals from the mother liquid, TS-1 crystals were redispersed in deionized water to make TS-1 zeolite sol. When TS-1 particles were dispersed in deionized water, there was no precipitation, presumably due to the Brownian motion of the nanosized TS-1 particles. Brownian motion of nano-sized particles enhances the dispersion of particles in the aqueous solution (Satoh and Kimura, 1994; Jung et al., 1996b). The sol behaves like TS-1 colloidal suspension.

Formation of TS-1 zeolite fiber

During the drying process of dispersed solution of TS-1 at 100°C, TS-1 particles were adsorbed on the inner surface of a glass test tube (1.5 (D)×10 (H) cm). Then the TS-1 fiber started to grow from the top toward the bottom as drying progressed at 100°C. Figure 3 shows an optical microphotograph and scanning electron microphotograph of the surface of the zeolite fiber. TS-1 fiber was formed with an average length of 2.5 mm, and the aspect ratio (L/D = length/diameter) was about 70. As shown in the electron microscope (Figure 3b), the sizes of the primary particles of TS-1 are in the 70–90-nm range. Those particles on the surface of zeolite fiber make highly ordered, two-dimensionally packed aggregates (Jung et al., 1996a). This two-dimensional packing was not observed when conventional micron-sized zeolite powder was used. The traditional powder sample showed randomly aggregated TS-1, which is quite different from the fiber. The fibers obtained are fragile, since the fiber consisted of agglomerates of TS-1 zeolite particles.

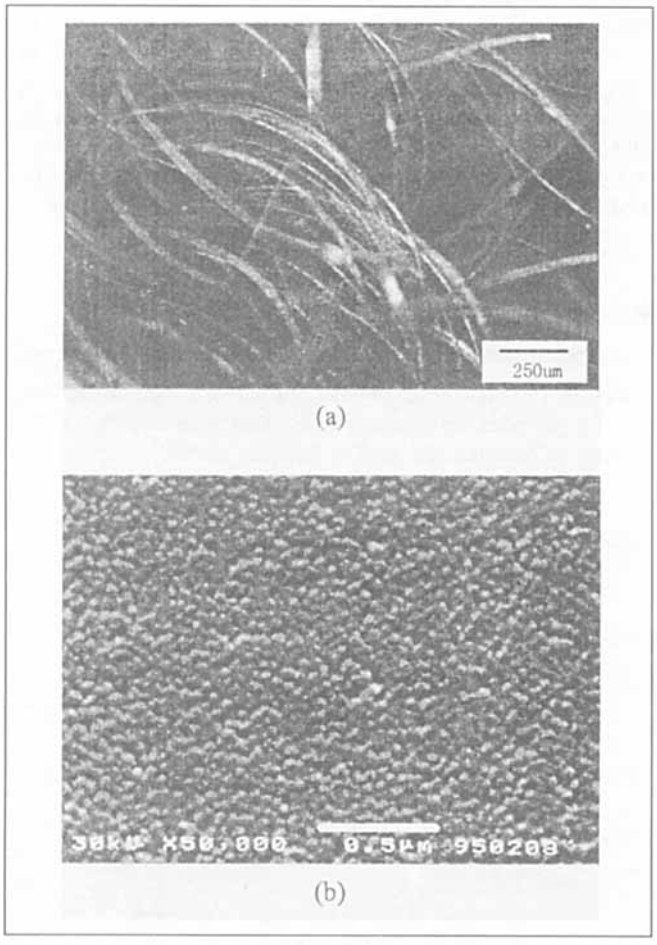

Figure 3. Optical microphotograph (a) and scanning electron microphotograph (b) of TS-1 zeolite fiber.

The effect of TS-1 solid content on the formation of fiber has been investigated by changing the TS-1 solid content from 0.1 wt. % to 50 wt. %. When the TS-1 solid content is less than 0.01 wt. % or more than 20 wt. %, TS-1 fiber is not formed. At the 5 wt. % solid content, the TS-1 fiber appears to be a yellowish color after drying at 100°C due to the remaining TPAOH on TS-1 fiber. As the TS-1 solid content increased from 0.02 wt. % to 5.0 wt. %, the aspect ratio increased from 30 to 200 and the aspect ratio of the TS-1 fiber exhibited the maximum value at 1.5 wt. % and dropped rapidly and the TS-1 contents increased (Jung et al., 1996b). These results suggest that the solid content of TS-1 greatly affects the formation of TS-1 fiber. In the sol-gel method, the particles with long shapes, or polymeric sol, have been known to be effective for fiber formation. However, TS-1 zeolite fiber was formed from spherical nanoparticles without the formation of long-shaped particles via a suitable redispersion-drying process. As the calcination temperature increased to 750°C, the Si MAS NMR spectrum peak at -102 ppm was seen to decrease. The peak at -102 ppm is assigned to the silanol group, which is present in the TS-1 as defect sites, or to protons, to compensate for the charge defect due to the presence of Ti ions in the lattice (Chapus et al., 1994). As we prepared well-crystallized TS-1 (> 95%) zeolite, the observed silanol groups were located mainly on the surface of the TS-1 nanocrystals before the thermal treatment. The decrease in the concentration of the silanol groups upon heating implies that the aggregated structure of nanosized zeolite was reinforced by the surface condensation of Si-OH on the TS-1 crystals through the thermal treatment (Jung et al., 1996a; Jung et al., 1997).

Formation of TS-1 zeolite film

TS-1 zeolite film has been prepared by dipping microslide glass directly into a dispersed TS-1 solution of 0.02 wt. %. Surface morphology of zeolite film has been investigated by atomic-force microscopy. The atomic-force microphotograph of the surface of the zeolite film (Figure 4a) clearly shows that TS-1 particles of size 80 nm are arranged on the surface of the microslide glass very much like the TS-1 zeolite fiber (Figure 3b). This suggests that the formation of film is similar to that of fiber. As shown in Figure 4b, the zeolite film was 0.5 μm thick. After calcinating the sample up to 550°C, there was apparently no micro- as well as no macrocrack on the surface of the TS-1 zeolite film. In addition, the zeolite film

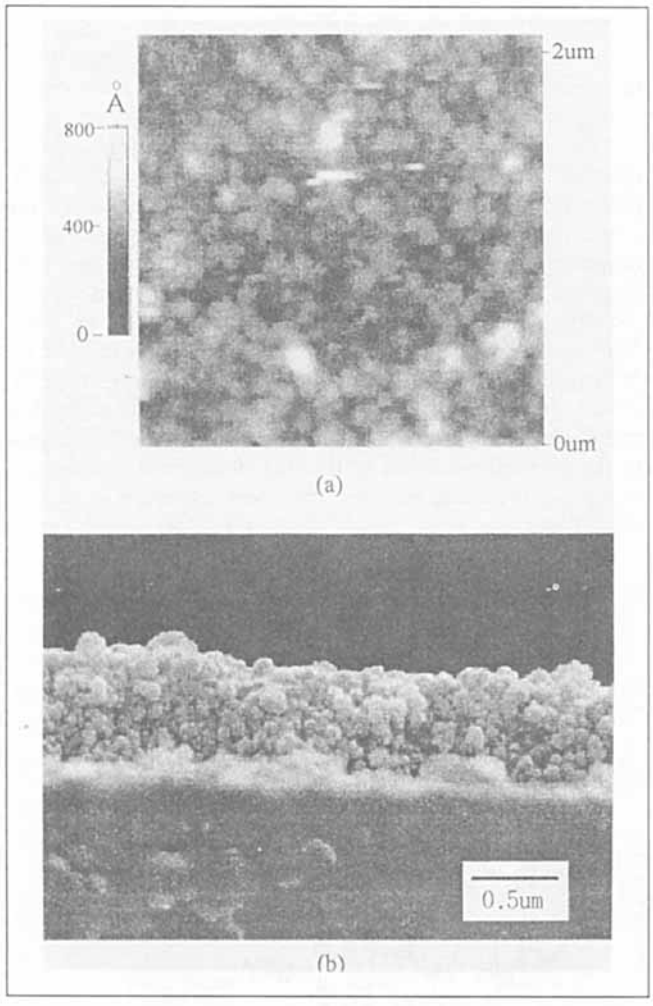

Figure 4. Atomic microforce (a) of the surface of TS-1 zeolite film and scanning electron microphotograph (b) of the fracture of TS-1 zeolite film.

shows optical transparency, as shown in Figure 5. As the solid content of TS-1 increased, a macrocrack was observed on the surface of the zeolite film. It was difficult to obtain thicker film by simply increasing the TS-1 solid content alone. However, thicker film could be obtained only by increasing the number of coatings. With more coatings, the film thickness was linearly increased up to 10 μm without micro-and macrocrack. Recently, Tsapatsis et al. (1995) synthesized zeolite L film in a petri dish by using nanosized zeolite particles. However, there is no report on the preparation of transparent TS-1 zeolite film from nanosized zeolite in the visible range. Schmidt et al. (1994) have suggested that high transparency can be obtained by using nanoscaled metals or ceramics as inorganic materials. The nanosized TS-1 particles (80 nm) are far below the visible light wavelength (400–700 nm). It seems there are few secondary large pores, which make zeolite film opaque, due to the dense packing of the TS-1 particles. Therefore, light does not scatter much when it passes through the TS-1 zeolite film. This transparent property of the film may be used for advanced optical materials (Srdanov et al., 1994).

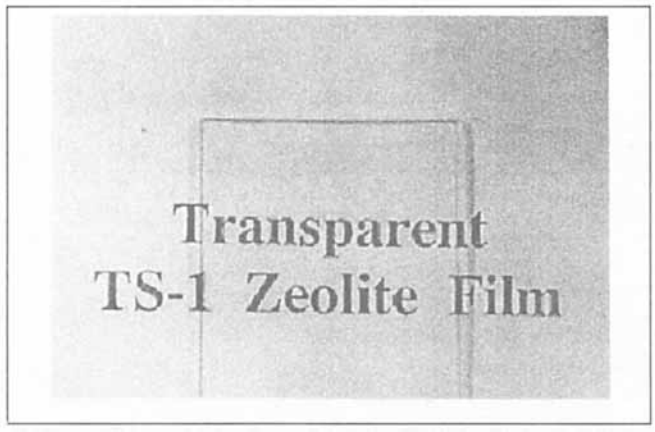

Figure 5. Optical microphotograph of TS-1 zeolite film after calcination at 550°C in air for 5 h.

Formation of the TS-1 zeolite monolith

Figure 6a shows the microphotograph of the TS-1 zeolite monolith after hydrothermal treatment at 170°C. After calcining at 550°C, the hydrothermally treated sample retains its

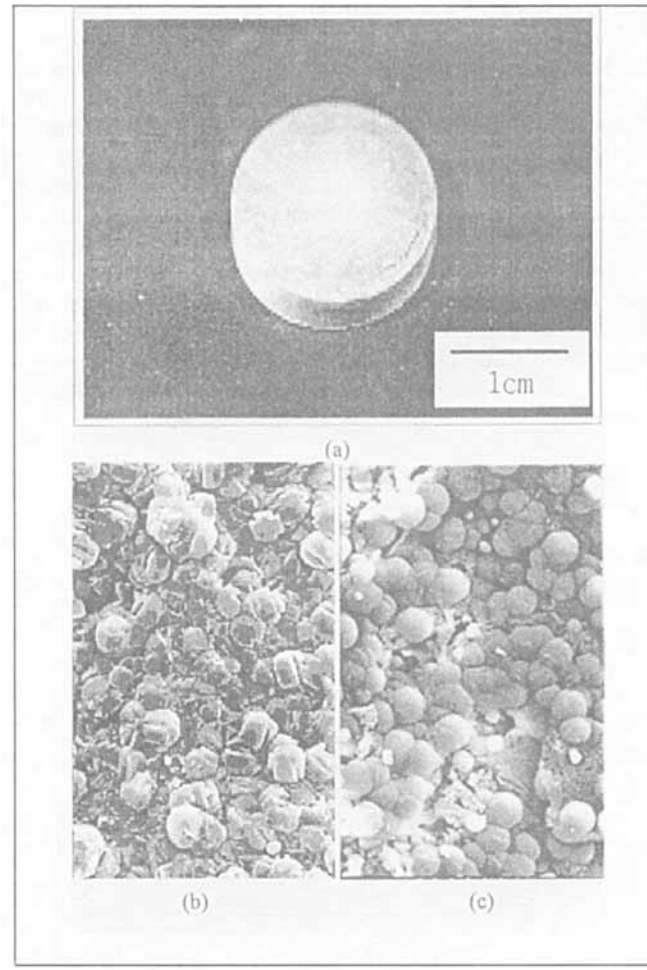

Figure 6. Optical microphotograph (a), scanning electron microphotograph of the surface (b), and fracture (c) of TS-1 zeolite monolith after hydrothermal treatment.

shape without cracks. In this process, heating of the sample should be slow to avoid cracks due to the rapid decomposition of TPAOH, the organic templating agent, in the monolith. It is expected that the zeolite monolith made up of zeolite may be applied to the separator, ion exchanger, reactor, and so forth, with high efficiency. When the pelletized cogel precursor is wetted by TPAOH and treated hydrothermally, an intergrown microstructure can be seen on the surface of monolith. This kind of intergrowth was also previously reported in a TS-1 crystallization (Tuel and Taarit, 1994) study and our previous work, the synthesis of ZSM-5 zeolite (Kiyozumi et al., 1996a).

The formation of cogel yields highly concentrated Ti-O-Si polymeric solid in the nanorange, and this acts as a nucleation site for TS-1 crystals. Upon hydrothermal treatment, nucleation and intergrowth of TS-1 proceeds from the surface and propagates into the center of the monolith. As shown in Figure 6b, the TS-1 crystals are intergrown, forming a randomly oriented structure. In this case, intergrowth of the TS-1 crystals at the grain boundary leads to the reinforcement of the monolith structure. The more uniform intergrowth enables the formation of a large zeolite monolith. A SEM image of the fracture in the monolith (Figure 6c), however, shows some amorphous phases inside the monolith that are not observed on the monolith surface.

The permeation rates of various gases through this monolith was measured at room temperature. Figure 7 shows the permeation results as a function of the square root of the reciprocal of the molecular weight. The permeability must be proportional to the square root of the reciprocal of the molecular weight, provided that the permeation occurs mainly in the Knudsen diffusion mechanism, while the plots for H_2 and He overlapped with a straight line, which suggested that the permeation of both gases occurred in the Knudsen diffusion regime (Matsukata et al., 1994; Lovallo and Tsapatsis 1996b). The Knudsen flow can be applied to gas separation from the mixture, like H_2 containing hydrocarbon (Kyozumi et al., 1996b). Further work is needed to make a perfect monolith in order to get a molecular sieving effect.

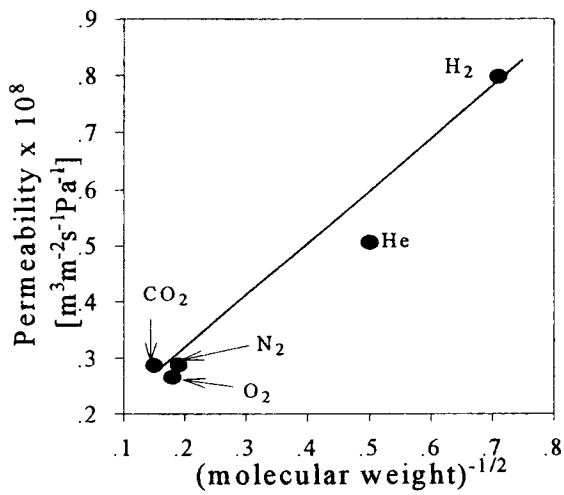

Figure 7. Changes of permeability of gases as a function of square root of the reciprocal of molecular weight.

Characterization of fiber, film, and monolith

In the present work the nanosized particles dispersed in the aqueous solution did not show severe aggregation or particle growth. During the drying and calcination processes, we can have various types of zeolite, fiber, film or monolith from the nano-TS-1 crystals. This is also observed in the sol-gel process from nanosol (Brinker and Scherer, 1990). In this sense, the morphological change in the TS-1 crystals should originate from the high surface reactivity of the nanoparticle. Figure 8 shows XRD patterns and FT-IR spectra of the zeolite fiber, film, and monolith, which were calcined at 550°C. This figure confirms that all forms of TS-1 zeolite have the MFI-type structure with an orthorhombic symmetry at 550°C. FT-IR spectra for calcined TS-1 fiber, film, and monolith at 550°C show a strong absorption band at 1100 cm^{-1} assigned to the internal vibration of the TO_4 tetrahedra. An absorption band at around 960 cm^{-1} has been observed in all samples. Taramasso et al. (1983), Tuel et al. (1993), and Deo et

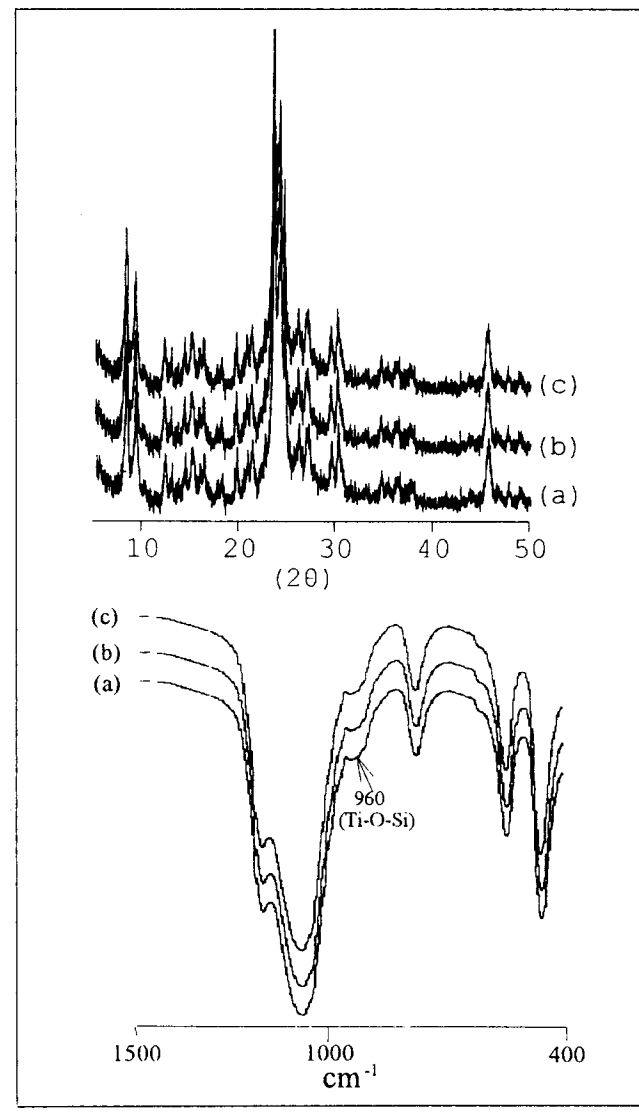

Figure 8. X-ray diffraction patterns and FT-IR spectra of TS-1 zeolite calcined at 550°C: (a) fiber, (b) film, and (c) monolith.

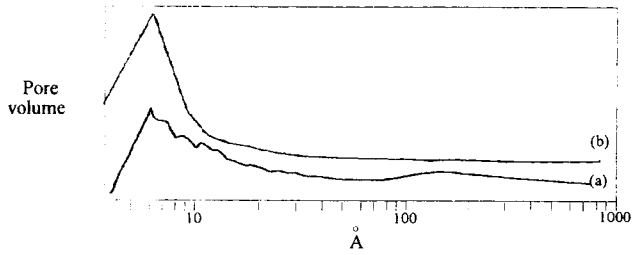

Figure 9. Pore-size distribution of TS-1 zeolite with calcination at 550°C: (a) fiber and (b) monolith.

al. (1993) also observed the appearance of a new band at 970 cm^{-1} when they incorporated Ti in the framework of highly dealuminated ZSM-5. Marra et al. (1994) have demonstrated that the IR band around 960 cm^{-1} exhibited by TS-1 zeolites can also be attributed to the stretching mode of a $[SiO_4]$ unit bonded to a Ti^{4+} ion (O_3SiOTi). After calcination of TS-1 fiber, there was no change of spectrum of the TS-1 fiber showing the thermal stability of the TS-1 structure.

Figure 9 shows the pore-size distribution of TS-1 zeolites. The TS-1 fiber exhibits two distinct peaks of pores with maximums at 7 Å and 170 Å after calcination at 550°C. The peak at 7 Å is assigned to the micropore of TS-1 zeolite structure (5.7 Å). This discrepancy of TS-1 pore size is probably a result of the detection limitations of our instrument (Fisson, Sorptomatic, 1990). The 170 Å peak comes from the secondary pores and is due to the fibrous aggregation of the TS-1 particles. This mesopore could be a distinctive aspect of the TS-1 zeolite fiber that was not observed in the monolith. It implies that the pore structure can be modified by a morphological change in the nano-TS-1 particles.

All the data show that a morphological design of the zeolites is also possible using nano particles similarly to sol-gel processing. An advanced application of zeolitic materials is mainly limited by the difficulty in morphological control, such as in fiber or film. It is therefore, expected that nanoapplication in zeolite can lead to new advanced materials in the future.

Conclusions

Nanosized titanium silicalite was prepared at atmospheric pressure and 80°C. Using mild conditions in hydrothermal synthesis allowed us to control the size of the TS-1 zeolite in the nanometer. TS-1 zeolite fibers, films, and monoliths were prepared by using the nanosized TS-1 zeolite. MFI structure is the structure of all the types of TS-1 zeolite manufactured in the present work.

It was found that the high reactivity of the nanosized TS-1 zeolite and the solid content of the TS-1 zeolite in aqueous solution play an important role in the formation of fiber and film. TS-1 zeolite monoliths made up of only particles of zeolite were obtained by hydrothermal treatment at 170°C for 3 days after pelletizing the nanosized precursor gel. Fiber and film of the TS-1 zeolite are shown to be optically transparent, and this property might be applicable to advanced optical materials.

Acknowledgment

This work was carried out with the financial support from the Daelim Engineering Co. and from the Yukong Co. Ltd.

Notation

H = height
cm^{-1} = wave number
°C = temperature

Literature Cited

Barrer, R. M., *Hydrothermal Chemistry of Zeolites*, Academic Press, London (1982).
Breck, D., *Zeolite Molecular Sieve*, Wiley, New York (1974).
Brinker, C. J., and G. W. Scherer, *Sol-Gel Science: The Physics and Chemistry of Sol-Gel Processing*, Academic Press, San Diego (1990).
Chapus, T., A. Tuel, B. Y. Taarit, and C. Naccache, "Synthesis and Characterization of Chromium Silicalite-1," *Zeolite*, **4**, 349 (1994).
Dong, J., T. Dow, X. Zaho, and L. T. Gao, "Synthesis of Membranes of Zeolite ZSM-5 and ZSM-35 by the Vapor Phase Method," *Chem. Soc. Chem. Commun.*, **16**, 1056 (1992).
Deo, G., A. M. Turek, and I. E. Wachs, "Characterization of Titania Silicalites," *Zeolites*, **13**, 365 (1993).
Elferink, W. J., B. N. Nair, R. M. Devos, K. Keizer, and H. Verweij, "Sol-Gel Synthesis and Characterization of Micro Porous Silica Membranes," *J. Colloid Interface Sci.*, **180**, 127 (1996).
Farrauto, R. J., and K. E. Voss, "Monolithic Diesel Oxidation Catalyst," *J. Appl. Catal. B.*, **10**, 29 (1996).
Grassi, M., R. Lapasin, and S. Pricl, "A Study on the Rheological Behavior of Scleroglucan Weal Gel Systems," *Carbohydr. Polym.*, **29**, 169 (1996).
Hayashi, K., M. Hirata, T. Katoh, and K. Kubota, "Antibacterial and Antifungal Dyed Synthetic Fiber," Japan Patent 119497 (1992).
Hennepe, H. J., C. D. Bargeman, M. H. V. Mulder, and C. A. Smolders, "Zeolite-Filled Silicone Rubber Membranes," *J. Memb. Sci.*, **35**, 39 (1987).
Hoffman, A. J., G. Mill, H. Yee, and M. R. Hoffmann, "Q-Sized CdS: Synthesis, Characterization, and Efficiency of Photoinitiation of Polymerization of Several Vinylic Monomer," *J. Phys. Chem.*, **96**, 5546 (1992).
Jia, M.-D., C. Baoshu, D. N. Richard, and J. L. Falconer, "Ceramic-Zeolite Composite Membranes and Their Application for Separation of Vapor/Gas Mixture," *J. Mem. Sci.*, **90**, 1 (1994).
Jung, K. T., J. H. Hyun, D. S. Kim, and Y. G. Shul, *Proc. of the Int. Congr. on Catalysis*, Baltimore, MD, p. 356 (1996a).
Jung, K. T., J. H. Lee, J. H. Hyun, D. S. Kim, and Y. G. Shul, *Proc. Int. Zeolite Conf.*, Seoul, Korea, p. 22 (1996b).
Jung, K. T., J. H. Hyun, Y. G. Shul, and D. S. Kim, "Synthesis of Fibrous Titanium Silicalite (FTS-1) Zeolite," *Zeolites*, in press (1997).
Kiyozumi, Y., S. Shin, Y. G. Shul, S. K. Ihm, and K.-K. Koo, "Crystal Growth of High Silica ZSM-5 at Low Temperature Synthesis Conditions," *Korean J. Chem. Eng.*, **13**, 144 (1996a).
Kiyozumi, Y., F. Mizukami, K. Maeda, M. Toba, and S. Niwa, "Synthesis of a Zeolite Film on a Mercury Surface," *Adv. Mater.*, **8**, 517 (1996b).
Lin, M. Y., H. M. Lindsay, D. A. Weitz, R. C. Ball, R. Klein, and P. Meakim, "University in Colloid Aggregation," *Nature*, **339**, 360 (1989).
Lovallo, T., and M. Tsapatisis, "Nanocrystalline Zeolites: Synthesis, Characterization and Application with Emphasis on Zeolite L Nanoclusters," *Advanced Techniques in Catalyst Synthesis*, W. R. Moser, ed., Academic Press, New York (1996a).
Lovallo, T., and M. Tsapatisis, "Preferentially Oriented Submicron Silicalite Membrane," *AIChE J.*, **42**, 3020 (1996b).
Marra, G. L., G. Tozzola, G. Leofanti, M. Padovan, G. Petrini, F. Genoni, B. Venurelli, A. Zecchina, S. Bordiga, and G. Ricchiardi, "Orthorhombic and Monoclinic Silicalites," *Zeolites and Related Microporous Materials in Studies in Surface Science and Catalysis*, Elsevier, Amsterdam, **84**, p. 559 (1994).
Matsukata, M., N. Nishiyama, and K. Ueyama, "Preparation of a Thin Zeolitic Membrane," *Zeolites and Related Microporous Materials, Studies in Surface Science and Catalysis*, Elsevier, Amsterdam, **84**, p. 1183 (1994).
Mintova, S., V. Valtchev, E. Vultcheva, and S. Veleva, "Crystallization Kinetics of Zeolite ZSM-5," *Zeolites*, **12**, 210 (1992).

Persson, A. E., B. J. Schoeman, J. Sterte, and J. E. Otterstedt, "Synthesis of Stable Suspension of Discrete Colloidal Zeolite (Na, TPA) ZSM-5 Crystals," *Zeolites*, **15,** 611 (1995).

Sano, T., Y. Kiyozumi, K. Maedea, M. Kawamura, T. Mouris, W. Inaoka, Y. Toida, and M. Watanabe, "Preparation and Characterization of ZSM-5 Zeolite Film," *Zeolites*, **11,** 842 (1992).

Satoh, N., and K. Kimura, "High-Resolution Solid State NMR in Liquis. 3. H-1-NMR Study of Organic Nano-Particles," *Chem. Lett.*, **11,** 2155 (1994).

Schmidt, H., "Multifunctional Inorganic-Organic Composite Sol-Gel Coating for Glass Surface," *J. Non-Cryst. Solids*, **178,** 302 (1994).

Schoeman, B. J., J. Sterte, and J.-E. Otterstedt, "The Synthesis of Colloidal Zeolite Hydroxysodalite Sol by Homogeneous Nucleation," *Zeolites*, **14,** 208 (1994).

Srdanov, V. I., N. P. Blake, D. Markgraber, H. Metiu, and G. D. Stucky, "Alkali Metal and Semiconductor Clusters in Zeolites," *Advanced Zeolite Science and Applications*, Vol. 85, *Studies in Surface Science and Catalysis*, Elsevier, Amsterdam, p. 115 (1994).

Taramasso, M., D. S. Milanese, G. Perrgo, B. Notari, and S. D. Milanese, "Preparation of Porous Crystalline Synthetic Material Comprised of Silicon and Titanium Oxides," U.S. Patent No. 4,410,501 (1983).

Thangaraj, A., M. J. Eapen, S. Sivanker, and P. Ratnasamy, "Studies on the Synthesis of TS-1," *Zeolites*, **12,** 943 (1992).

Tsapatisis, M., M. Lovallo, T. Okubo, M. E. Davis, and M. Sadakata, "Characterization of Zeolite L Nanoclusters," *J. Chem. Mater.*, **7,** 1734 (1995).

Tuel, A., and B. Taarit, "^{13}C Solid-State n.m.r. Investigation of TS-1/TS-2 Intergrowth Structures," *Zeolites*, **14,** 169 (1994).

Tuel, A., B. Taarit, and C. Naccache, "Characterization of TS-1 Synthesized Using Mixtures of Tetrabutyl and Tetraethyl Ammonium Hydroxides," *Zeolites*, **13,** 454 (1993).

Uguina, M. A., D. P. Serrano, G. Ovejero, R. Van Grieken, and M. Camacho, "Preparation of TS-1 by Wetness Impregnation of Amorphous SiO_2-TiO_2 Solids," *J. Appl. Catal. A*, **124,** 391 (1995).

Valtchev, V., S. Mintova, B. Schoeman, L. Spasov, and L. Knostantinov, "Zeolite Crystallization on Mullite Fibers," *A Refined Tool for Designing Catalytic Sites*, Vol. 97, *Studies in Surface Science and Catalysis*, Elsevier, Amsterdam p. 527 (1995).

Yan, Y., M. E. Davis, and G. R. Gavalas, "Preparation of Zeolite ZSM-5 Membrane by in situ Crystallization on Porous α-Al_2O_3," *Ind. Eng. Chem. Res.*, **34,** 1562 (1995).

Yamamura, M., K. Chake, T. Wakatsuki, H. Okado, and K. Fujimoto, "Synthesis of ZSM-5 with Small Crystal Size and its Catalytic Performance for Ethylene Oligomerization," *Zeolites*, **14,** 643 (1994).

Manuscript received Oct. 28, 1996, and revision received Apr. 4, 1997.